The effects of surface temperature on the gas-liquid interfacial reaction dynamics of $O(^3P)$+squalane

Cite as: J. Chem. Phys. **122**, 024712 (2005); https://doi.org/10.1063/1.1835268
Submitted: 11 September 2004 • Accepted: 27 October 2004 • Published Online: 23 December 2004

Sven P. K. Köhler, Mhairi Allan, Hailey Kelso, et al.

The effects of surface temperature on the gas-liquid interfacial reaction dynamics of $O(^3P)$+squalane

Sven P. K. Köhler, Mhairi Allan, Hailey Kelso, David A. Henderson, and Kenneth G. McKendrick
School of Engineering and Physical Sciences, Heriot-Watt University, Edinburgh EH14 4AS, United Kingdom

(Received 11 September 2004; accepted 27 October 2004; published online 23 December 2004)

OH/OD product state distributions arising from the reaction of gas-phase $O(^3P)$ atoms at the surface of the liquid hydrocarbon squalane $C_{30}H_{62}/C_{30}D_{62}$ have been measured. The $O(^3P)$ atoms were generated by 355 nm laser photolysis of NO_2 at a low pressure above the continually refreshed liquid. It has been shown unambiguously that the hydroxyl radicals detected by laser-induced fluorescence originate from the squalane surface. The gas-phase OH/OD rotational populations are found to be partially sensitive to the liquid temperature, but do not adapt to it completely. In addition, rotational temperatures for OH/OD($v'=1$) are consistently colder (by 34 ± 5 K) than those for OH/OD($v'=0$). This is reminiscent of, but less pronounced than, a similar effect in the well-studied homogeneous gas-phase reaction of $O(^3P)$ with smaller hydrocarbons. We conclude that the rotational distributions are composed of two different components. One originates from a direct abstraction mechanism with product characteristics similar to those in the gas phase. The other is a trapping-desorption process yielding a thermal, Boltzmann-like distribution close to the surface temperature. This conclusion is consistent with that reached previously from independent measurements of OH product velocity distributions in complementary molecular-beam scattering experiments. It is further supported by the temporal profiles of OH/OD laser-induced fluorescence signals as a function of distance from the surface observed in the current experiments. The vibrational branching ratios for $(v'=1)/(v'=0)$ for OH and OD have been found to be (0.07 ± 0.02) and (0.30 ± 0.10), respectively. The detection of vibrationally excited hydroxyl radicals suggests that secondary and/or tertiary hydrogen atoms may be accessible to the attacking oxygen atoms. © *2005 American Institute of Physics.* [DOI: 10.1063/1.1835268]

I. INTRODUCTION

In contrast to the dynamics of interfacial reactions between gas-phase species and solids, which have been thoroughly investigated over an extended period,[1,2] those at the gas-liquid interface have been studied far less. Recently, this situation has begun to change. A number of serious dynamical investigations of gas-liquid interfacial inelastic scattering have now been conducted.[3–5] To a still more limited extent, the very first explorations of the dynamics of gas-liquid reactive scattering have begun.[6–8] In this paper, we attempt to add momentum to these developments. We report a different, spectroscopically based, dynamical investigation of one representative system, the reaction of gas-phase ground state $O(^3P)$ atoms at the surface of the long-chain liquid hydrocarbon squalane, $C_{30}H_{62}$. Despite a lack of understanding of their dynamics, gas-liquid interfacial reactions are clearly important in a wide variety of fields. These would broadly include biological processes such as respiration, industrial applications such as distillation, and many atmospheric phenomena at the surface of the sea or of suspended aerosol droplets. For example, in the lower atmosphere, the accumulation of even modest amounts of organic material by aqueous aerosol particles leads to the development of an outer, hydrophobic layer. This organic material presents the first barrier to exchange or reaction with atmospheric gases, including the key highly reactive free radical species such as OH. A number of experiments[9–11] have recently been directed towards the kinetics of reactions with mimics of these surfaces.

A related technological problem involving reaction between $O(^3P)$ and solid (rather than liquid) condensed organic phases has been discovered at much higher altitudes in the atmosphere. Between ~200 and ~700 km, $O(^3P)$ is the most abundant oxygen species. This is the relevant range of altitudes for spacecraft in low-earth orbit. Due to the orbital motion, the collisions between the craft and (effectively stationary) atmospheric constituents have relatively high energies, resulting in serious erosion of organic polymeric materials. It has been demonstrated, for example, that collisions with $O(^3P)$ atoms with an energy of around 450 kJ mol^{-1} can lead to the degradation of polymeric heat shields.[12]

Early experimental studies between gas-phase species and liquids were aimed at the determination of the stable products formed in the liquid phase. Among those most directly relevant to the present work, Hori *et al.* performed experiments on $O(^3P)$ atoms reacting with various homogeneous liquid-phase hydrocarbons in which they were generated. They found that alcohols were the main stable products.[13] Moving yet closer to the target of the current work, Zadok and Mazur[14] and Patiño *et al.*[15] detected the

products in the liquid phase after reaction between gas-phase oxygen and liquid hydrocarbons. They also found alcohols to be the main products. Not surprisingly, all these experiments revealed that the reactivity of the hydrocarbon decreases in the order tertiary>secondary>primary. This result simply reflects the relative bond energies, with a similar effect being observed in the corresponding homogeneous gas-phase reaction.[16,17] Related experiments using more modern direct spectroscopic methods by Naaman and co-workers on the reaction between $O(^3P)$ atoms and cyclohexane clusters took a step from the opposite direction along the transition from pure gas-phase experiments to those in the liquid phase.[18]

Finally, and most significantly, experiments most closely related to those reported here have succeeded in detecting scattered gas-phase species for the same gas-liquid interfacial system using complementary molecular-beam techniques. An oxygen atom beam was directed onto the surface of liquid squalane and gas-phase products detected by time-of-flight mass spectrometry. Inelastically scattered oxygen atoms, the reactive products hydroxyl radicals, and water were the main species detected. They were all found to have a bimodal kinetic energy distribution, for proposed mechanistic reasons that are discussed further below in the context of our own results.

An important aspect of our mechanistic discussions will be an appeal to the benchmark of the dynamics of the corresponding homogeneous gas-phase reactions between $O(^3P)$ and smaller hydrocarbons. Fortunately, these systems have been very well studied and the key features of their dynamics are considered to be relatively well understood.[19] The pioneering work by Andresen and Luntz[20] on various hydrocarbons revealed the rotational distribution of the OH radicals to be generally cold. The reactivity increases in the order methane<primary<secondary<tertiary, for the same energetic reasons noted above for liquid-phase reactions. This is also found, as expected, to correspond to the sequence in which the OH vibrational branching ratio $(v'=1)/(v'=0)$ increases. Further experimental work by Whitehead,[21] McKendrick,[22,23] and Kajimoto[24] has extended this field. A review has been published recently.[19] It has been concluded that the generally cold rotational distribution is the result of a near-linear transition state through which the oxygen atom abstracts a hydrogen atom. This mechanism is also confirmed by extensive theoretical calculations which have accompanied the experimental efforts over the years.[25–32]

In contrast, there has not been an equivalent level of theoretical effort on the dynamics of the interfacial reaction between oxygen atoms and liquid hydrocarbons. There has been some related work on the structure of the liquid surface. Harris[33] has reported molecular dynamics simulations of the structure of the liquid-vapor interface of straight-chain *n*-eicosane, $C_{20}H_{42}$, and *n*-decane, $C_{10}H_{22}$. More recently, Siepmann and co-workers have examined squalane itself using similar methods.[34] Perhaps the closest theoretical dynamical studies are trajectory calculations of the reaction between $O(^3P)$ atoms and a self-assembled monolayer (SAM) surface. Independent work of this type has been reported by Hase and co-workers[35] and Troya and Schatz.[36,37] The relevant potential energy surface was constructed from a quantum mechanics/molecular mechanics (QM/MM) (MM) model. The outer hydrocarbon groups and the oxygen atom were treated in a QM fashion whereas the remaining atoms in the SAM were represented by MM functions. Such SAM surfaces can serve as a well-ordered model of other condensed-phase hydrocarbons, a feature now also being exploited experimentally in inelastic scattering,[38–40] the kinetics of degradation,[41,42] and related attack by ionic species.[43]

We present here dynamical results on the reaction between $O(^3P)$ atoms and the liquid hydrocarbon squalane $C_{30}H_{62}$ and, for technical reasons, the fully deuterated analogue, $C_{30}D_{62}$. This follows our earlier brief letter,[44] in which we described the first limited spectroscopic measurements of internal energy distributions of the OD gas-phase product from the fully deuterated squalane surface. We report here on a full systematic investigation of the internal energy distributions of the OD and OH products. Importantly, we have also studied the effects of varying the surface temperature on the gas-phase product state distributions. We infer additional information from simulations of recorded appearance time profiles. Our aim is to infer dynamical insight into the mechanism of this gas-liquid interfacial process.

II. EXPERIMENT

The experimental setup has only been described very briefly elsewhere[44] and therefore a more complete description is given here. A device based around a rotating stainless-steel wheel, similar in concept to those described previously,[3,6,45,46] is used to create a continuously refreshed liquid hydrocarbon surface. The rotating wheel of 5 cm diameter is immersed in a copper bath filled with the liquid hydrocarbon squalane, as illustrated in Fig. 1(a). A Teflon® spacer is placed in front of the wheel to ensure good coverage of its front surface. We found this arrangement to be more effective for small sample volumes than metal knife-edge scrapers.[3,6,45] The bath is temperature controlled by a Peltier element to allow temperature-dependent measurements. The temperature of the bath was typically maintained at $-10\,^{\circ}\mathrm{C}$ for low-temperature and at $+80\,^{\circ}\mathrm{C}$ for high-temperature experiments. The effect this has on the temperature of the liquid on the surface of the wheel when the system is under vacuum cannot be established directly in our current arrangement. We have, however, verified in independent tests performed on the open bench (where any heat losses should, if anything, be greater than under vacuum) that the surface temperature of the liquid-covered wheel is $\geqslant 60\,^{\circ}\mathrm{C}$ at the higher and $\leqslant 0\,^{\circ}\mathrm{C}$ at the lower temperature. We are confident therefore that we are able to span a temperature range of at least 60 K. Some ''thermal'' calibration measurements, explained further below, were also performed at room temperature $(297\pm 3\ \mathrm{K})$.

The partially branched hydrocarbon squalane (2,6,10,15,19,23-hexamethyltetracosane) was chosen due to its convenient low melting point and very low vapor pressure of $\sim 1\times 10^{-7}$ Torr at room temperature. It has been established as something of a benchmark system for related experiments on long-chain liquid hydrocarbons.[3–8,44] As previously reported, we used a commercial sample of fully

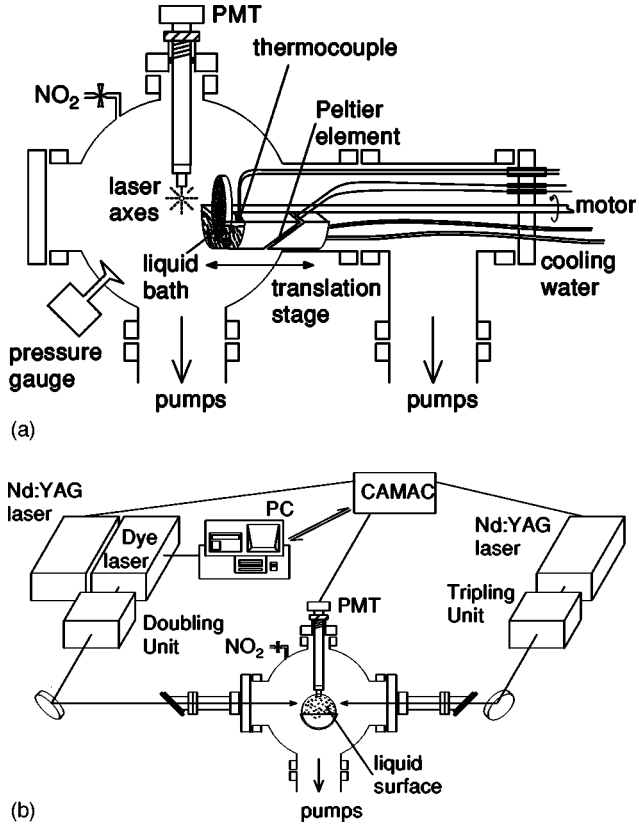

FIG. 1. (a) Side elevation of experimental chamber with translation stage and electrical and optical feedthroughs. (b) Front elevation of experimental chamber with optical detection system. Photolysis and probe lasers counter-propagate a selected distance in front of the liquid surface.

deuterated squalane $C_{30}D_{62}$ (C/D/N Isotopes Inc., isotope enrichment 99.3 at. %) for selected measurements.

The liquid-surface assembly was contained in a custom-built vacuum chamber, shown schematically in Fig. 1(a), surrounded by the remaining optical and data-collection components of the apparatus, as indicated in Fig. 1(b). The third harmonic of a Nd:YAG laser (Continuum Surelite SLII-10) with a typical energy of 120 mJ in a $\sim$5 ns pulse at 355 nm propagated at a selected distance, typically in the range 4–15 mm, above the liquid surface. This generated $O(^3P)$ atoms from bulk phase NO_2 (BOC, 98.3%) admitted into the chamber at a pressure of typically 1.0 mTorr. The laser polarization was selected to optimize the fraction of the moderately anisotropic angular distribution of $O(^3P)$ atoms recoiling towards the surface.[47] The oxygen atom speed distribution is broad with an average speed of 1340 $m\,s^{-1}$ and an average collision energy of 15.8 $kJ\,mol^{-1}$ in the laboratory frame (i.e., if the surface is treated as infinitely massive). However, earlier experiments[6–8] show that an effective surface mass that depends on the oxygen kinetic energy can be assigned to the squalane surface as will be discussed further below.

A fraction of the oxygen atoms abstract hydrogen atoms. The resulting hydroxyl radicals were detected in the gas phase by laser-induced fluorescence (LIF) on the well-known A-X band. The LIF was excited by the frequency-doubled output of a Nd:YAG (Spectron Laser Systems SL803S) laser-pumped dye laser (Spectron Laser Systems SL4000G, SL4000EX). The probe beam counter-propagated the photolysis beam, cocentered the same distance above the surface. The typical maximum probe pulse energy was $\sim$1 mJ in a $\sim$5 ns pulse, reduced to $\sim$0.5 mJ during the measurements of vibrational branching ratios to minimize the effects of differential optical saturation. The fluorescence was collected using a commercial liquid light guide (Ultrafine Technology Series 300) placed $\sim$10 mm above the common laser axis.

Depending on the particular experiment, lines in the (1,0), (1,1), and (2,1) bands of OH or OD were excited. Fluorescence on selected emission bands was isolated using custom interference filters [center wavelength 317 nm, full width at half maximum (FWHM) 8 nm]. In most cases, this was the respective diagonal (1,1) or (2,2) band. In measurements of the vibrational branching ratio, the inconvenience of upper state predissociation for OH was tolerated in exchange for the significant advantages of using (1,0) and (2,1) bands of similar strength that are also relatively close in wavelength. The reduced fluorescence quantum yields for even the lowest rotational levels of OH $A\,^2\Sigma^+$ $(v'=2)$ then had to be taken into account in the analysis.[48,49] OH $A\,^2\Sigma^+$ $(v'=1)$ is not significantly predissociated in the lower rotational levels of interest in this work, as are none of the relevant vibronic levels of OD. For the purposes of deriving rotational populations of $OH(v''=1)$, it was found that the signal-to-noise was superior for those excited on the diagonal (1,1) band with fluorescence collected on the (1,0) band (bandpass filter with center wavelength 280 nm, FWHM 10 nm). Exciting the (2,1) band remained more convenient for $OD(v'=1)$. The (1,0) bands were used to obtain rotational populations for $(v'=0)$ of both OH and OD. Fluorescence transmitted through the interference filter was detected by a photomultiplier tube. The waveform was captured by a transient digitizer incorporated in a CAMAC (IEE488) modular data acquisition system. Signals were in all cases collected in a gate of length 1.8 μs starting 150 ns after the probe laser pulse to discriminate against scattered laser light. Processing and analysis were carried out on a microcomputer, running custom-written LABVIEW® software. This also provided control, via appropriate modules, of other experimental parameters such as relative timings and the probe laser wavelength.

III. RESULTS

A. Verification of authentic nascent products from the gas-liquid interfacial reaction

Clearly, verification that any observed OH signals are the result of $O(^3P)$ reacting at the squalane surface is crucial. Equally, the validity of any mechanistic conclusions inferred from observed product state distributions relies on these populations being nascent, unmodified by secondary collisions in the gas phase.

The authenticity of the OH LIF signals has been confirmed in two ways. Establishing this point was a major part of the motivation for acquiring a fully deuterated sample of squalane. As described in our previous communication,[44] the observation of the product OD from this sample is very strong evidence for a reaction taking place at the surface.

The naturally abundant levels of deuterium in any gas-phase impurities are obviously negligible. We also see no evidence for isotope exchange between the deuterated squalane and any gas-phase compounds that might have given rise to either prompt photolytic or spurious homogeneous bimolecular OD production.

The confirmation through isotopic labeling is corroborated by the observed time dependence of the appearance of the OD LIF signals from deuterated squalane, as reported previously,[44] or of OH from normal squalane, which we report here. For normal squalane, we do indeed see a spurious, prompt, photolytically produced OH LIF signal. We assign it to the hydrogen-containing impurity, probably a nitrogen oxoacid, widely found previously[22] to be a contaminant of commercial supplies of NO_2. This OH signal has its maximum value immediately following the photolysis pulse. It decays rapidly to zero over a period of a few microseconds, consistent with fly out of a relatively high velocity photodissociation product. Crucially, its appearance is identical regardless of the distance of the photolysis and probe beams from the liquid surface. In contrast, the character of the additional OH signal which appears at later times is strongly dependent on this distance, mirroring the behavior of the only type of OD signal seen from deuterated squalane.

It is therefore possible, if desired, to remove with confidence the spurious photolytic OH signal by subtracting the initial component of a trace recorded with a large beam-to-surface distance from those at shorter distances. In practice, the subtracted signal had a peak intensity of only ~15% of that of the authentic signal at the shortest distances. Examples of the residual, distance-dependent traces are shown in Fig. 2. These show unmistakable features characteristic of an interfacial reaction. There is an initial ''dead time'' during which there is no reactive OH product. This is followed by a sharp onset of the signal, at a time that is correlated with the round-trip distance to and from the surface. The magnitude of the peak OH signal also declines, as expected for straightforward geometric reasons, as the distance increases. We discuss more quantitatively below the relationship of these features to the known $O(^3P)$ and anticipated OH velocities.

For either OH or OD, therefore, we are entirely confident that the LIF signal at the peak of ~10–15 μs and the shortest practical distance of ~4 mm results entirely from reaction at the surface. The separate question is whether this represents a nascent sample. This obviously depends on the pressure at which the measurement is made. With this in mind, we have chosen a standard value of 1.0 mTorr to conduct ''nascent'' measurements.

Assuming a typical gas-kinetic total collision rate constant of $\sim 10^7$ Torr^{-1} s^{-1} (or $\sim 3\times 10^{-10}$ cm^3 s^{-1}), the average number of collisions per molecule experienced during the full period of 15 μs is only ~0.15. Alternatively, and perhaps more persuasive since it does not rely on an assumption of thermal velocities, the mean-free path can be estimated on the basis of a reasonable collision cross section of 0.35 nm^2 for either O or OH with NO_2. This gives a mean-free path of ~9 cm, which is also approximately an order of magnitude longer than the distance between liquid surface and the laser beam axis.

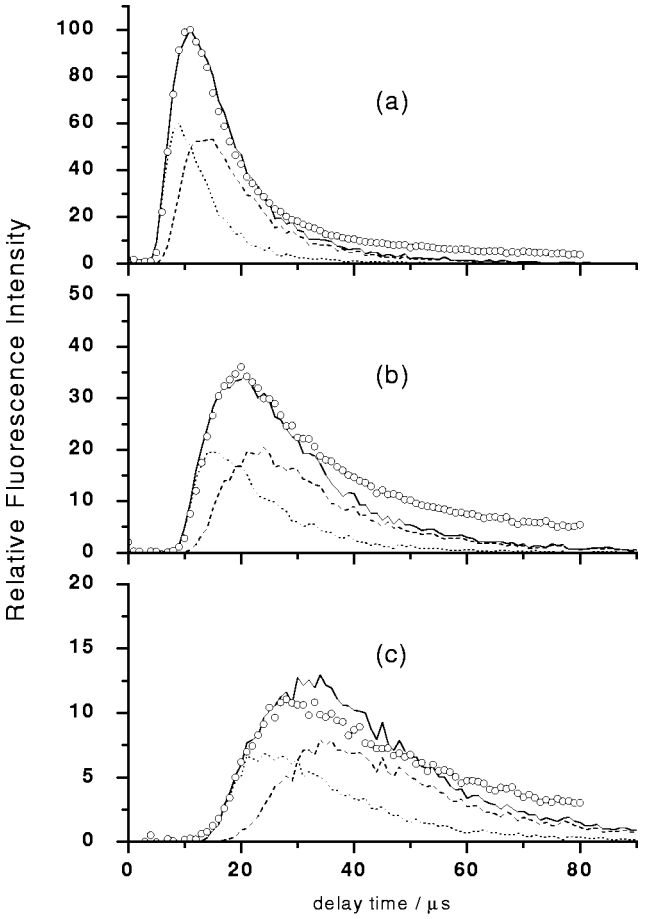

FIG. 2. Measured and simulated appearance profiles of the OH radical [recorded by LIF on the $Q_1(1)$ line of the (1,0) band] after reaction of $O(^3P)$ atoms with a liquid squalane surface. Open circles are experimental measurements, solid lines are the combined simulations, and the dotted and dashed lines are the direct and thermal component, respectively (as discussed in the text). Liquid temperature = 298 K; $p(NO_2) = 1$ mTorr; distance surface-probe laser: (a) 4.5 mm, (b) 8 mm, and (c) 13 mm.

B. Effect of surface temperature on product rotational distributions

We have previously reported[44] measurement of nascent gas-phase OD LIF spectra from reaction of $O(^3P)$ atoms with a liquid surface of fully deuterated squalane at a single fixed temperature ($-10\,^\circ$C). We present here the systematic investigation of the reaction dynamics of $O(^3P)$ atoms with both fully deuterated and ''normal'' squalane at two different temperatures. We have verified above that either the OH or OD radicals detected typically ~12 μs after the photolysis laser are solely the product of reactive scattering of $O(^3P)$ atoms with the squalane surface. Unambiguous and readily analyzable OH LIF spectra were recorded under these conditions. A representative spectrum of nascent OH radicals is shown in Fig. 3. This has a typical signal-to-noise greater than 100.

We chose not to attempt to derive rotational distributions directly from the measured spectra using known or estimated line strength and other detectivity factors. To avoid rotational-level dependent effects that influence the detection sensitivity, a more reliable relative calibration method was used. This was based on supplementary thermal spectra re-

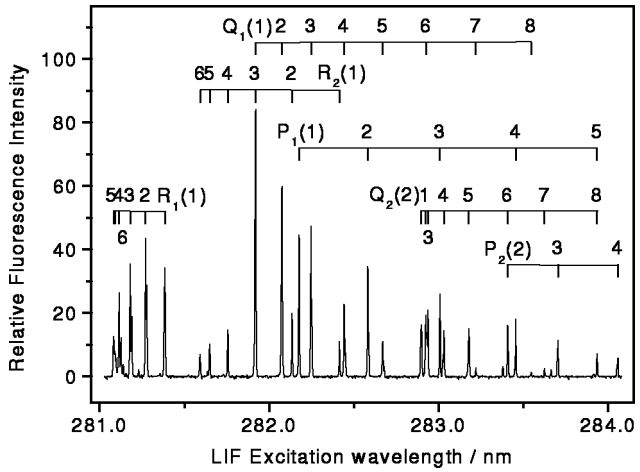

FIG. 3. Representative OH A-X (1,0) LIF excitation spectrum recorded after reaction of $O(^3P)$ with the liquid surface of squalane, $C_{30}H_{62}$. Collection time ≈ 2 h. Liquid temperature $\geqslant 333$ K; $p(NO_2)=1$ mTorr; photolysis-probe delay $=10$ μs; distance surface-probe laser $=4$ mm.

corded alternately with the nascent spectra. For the thermal spectra, a further 50 mTorr N_2 was added to the chamber and the time delay between photolysis and probe increased to ~ 30 μs. The average number of collisions that the hydroxyl radicals undergo correspondingly increases by a factor of ~ 100 to ~ 15 collisions under thermal conditions. N_2 is known to be an effective rotational quencher of OH (Ref. 50) and we therefore believe that the hydroxyl radicals adopt a rotational distribution essentially identical to that of a thermally equilibrated sample. Since the populations are therefore trivially calculable from Boltzmann statistics, the ratio of signals in the nascent and thermal spectra can then be used to deduce relative populations under nascent conditions. We have measured rotational populations for both OH and OD in each of the F_1 and F_2 spin-orbit manifolds for both $(v'=0)$ and $(v'=1)$ at two different temperatures. Figure 4 shows, as an example, the rotational populations of the nascent OH radicals in the F_1 manifold after collision with the liquid squalane surface kept at $\leqslant 0\,^\circ$C and at $\geqslant +60\,^\circ$C. These populations are compared with those found previously[22,51] for the pure gas-phase reaction between $O(^3P)$ atoms and cyclohexane C_6H_{12}. It is clear from this figure that the rotational populations of the OH radicals originating from the "cold" ($\leqslant 0\,^\circ$C) surface are colder than those originating from the "hot" ($\geqslant +60\,^\circ$C) one. One can also see that the rotational distribution in $OH(v'=1)$ is colder than that in $OH(v'=0)$. This effect is apparently not as pronounced, though, as it is in the gas-phase reaction with cyclohexane.[22,51]

Differences between the various population distributions are more readily characterized by presenting the data in the form of a Boltzmann plot. As these turn out to be approximately linear in all cases, it is also possible to assign a single nominal temperature which provides a convenient comparison with the liquid-surface temperature.

Figure 5 shows Boltzmann plots for the F_1 manifolds in each of the vibrational levels of OH from reaction with the liquid surface. The plots show that the rotational temperatures of the hydroxyl radicals, at least at this particular time

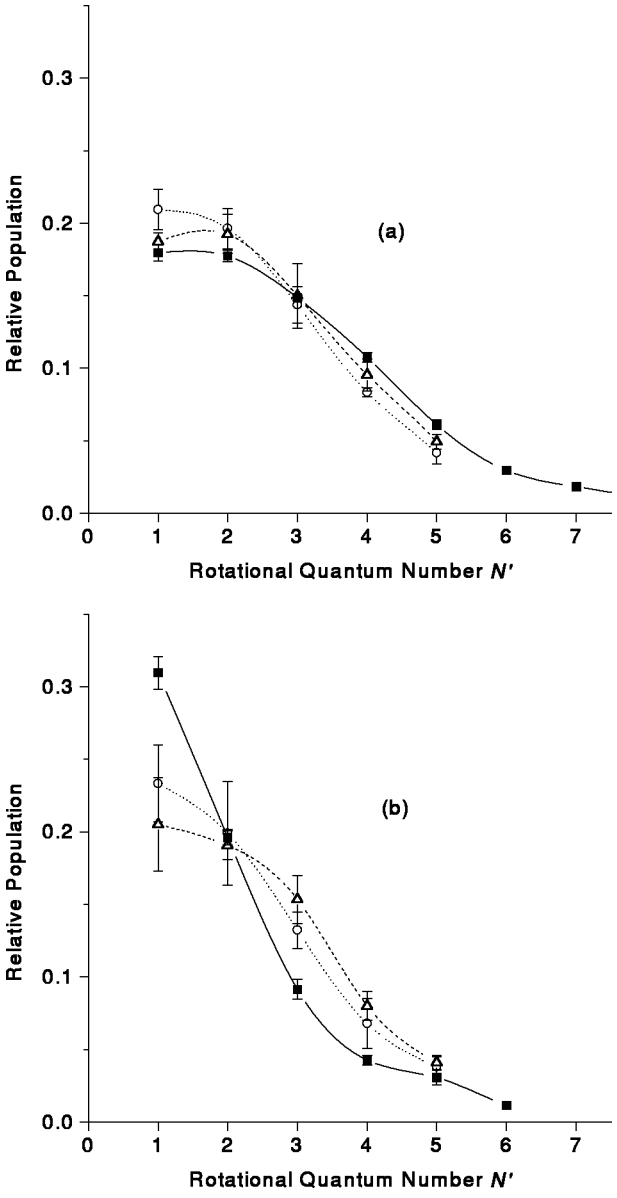

FIG. 4. Rotational populations in the F_1 manifold of OH in (a) $v'=0$ and (b) $v'=1$ after reaction of $O(^3P)$ with a liquid squalane surface at a temperature $\leqslant 273$ K (open circles) and $\geqslant 333$ K (open triangles) in comparison with results from Ref. 23 for the homogeneous gas-phase reaction between $O(^3P)$ and cyclohexane (filled squares). $p(NO_2)=1$ mTorr; photolysis-probe delay $=10$ μs; distance surface-probe laser $=4$ mm.

delay near the peak of their appearance (see Fig. 2), are influenced by the surface temperature. In all cases, the product rotational temperature increases with increasing surface temperature. However, the hydroxyl radicals clearly do not adopt the surface temperature completely. The average differences in rotational temperature are 38 ± 5 K whereas the surface temperatures differ by at least 60 K. Furthermore, the rotational temperatures in $(v'=1)$ are consistently colder than those in $(v'=0)$. As noted above, though, the magnitude of this temperature difference $(34\pm 5$ K) is considerably less than that in homogeneous gas-phase experiments with cyclohexane (~ 180 K).

Table I collects all rotational temperatures derived in this systematic investigation. None of them differ significantly

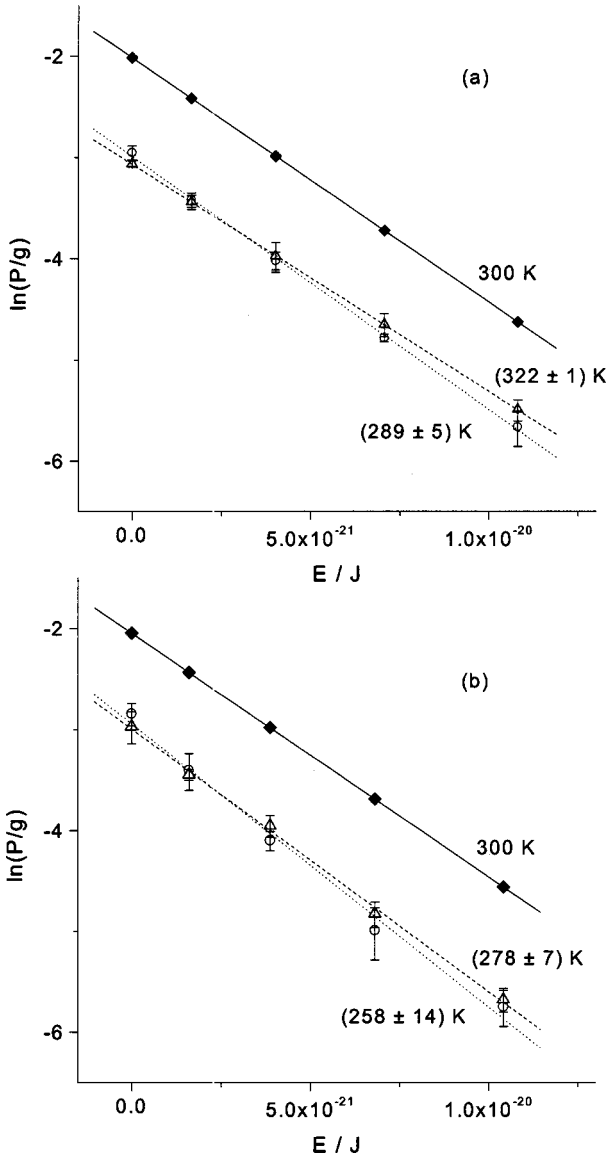

FIG. 5. Boltzmann plots for the F_1 manifold of OH in (a) $v'=0$ and (b) $v'=1$. Open circles correspond to OH products after reaction of $O(^3P)$ atoms with a liquid squalane surface at a temperature $\leqslant 273$ K, open triangles to a surface temperature $\geqslant 333$ K. Filled squares are the results of thermal spectra assumed to be equilibrated at 300 K and are offset for clarity. $p(NO_2)=1$ mTorr; photolysis-probe delay $=10\ \mu$s; distance surface-probe laser $=4$ mm.

between the F_1 and F_2 manifolds. The fine-structure and Λ-doublet populations also do not deviate significantly from thermal populations.

C. Product vibrational branching

We have confirmed our previous qualitative observation[44] of a significant branching fraction for vibrationally excited OD radicals from the deuterated squalane sample. We also report here the detection of OH$(v'=1)$ from a normal squalane sample, and make a quantitative assessment of the vibrational branching ratios in both cases. These ratios were derived by measuring the relative intensities of a number of lines in a pair of bands originating from either $(v'=0)$ or $(v'=1)$, respectively. The probe laser pulse energy was kept constant at the pairs of respective wavelengths. Transition probabilities in absorption and emission, fluorescence quantum yields due to predissociation, and emission wavelength-dependent interference filter sensitivity were taken into account. The resulting $(v'=1)/(v'=0)$ vibrational branching ratio are 0.30 ± 0.10 for OD and 0.07 ± 0.02 for OH. We do not regard the larger branching ratio for OD than for OH as surprising. This is as would be expected, in the absence of any other strong dynamical constraints, because of the quite substantial difference in the vibrational energy spacing.

TABLE I. Rotational temperatures (in K) measured for OH on the (1,0) and (1,1) bands and OD on the (1,0) and (2,1) bands in both the F_1 and F_2 manifolds after reactive scattering of $O(^3P)$ atoms with a liquid squalane surface at either $\leqslant 273$ K or $\geqslant 333$ K. Photolysis-probe delay $=10\ \mu$s; $p(NO_2)=1$ mTorr.

Surface temperature (K)		$(v'=0)$		$(v'=1)$	
		$\leqslant 273$	$\geqslant 333$	$\leqslant 273$	$\geqslant 333$
OH	F_1	289 ± 5	322 ± 1	258 ± 14	278 ± 7
	F_2	308 ± 15	341 ± 11	246 ± 11	280 ± 19
OD	F_1	279 ± 6	305 ± 6	264 ± 10	299 ± 7
	F_2	277 ± 5	311 ± 4	239 ± 8	284 ± 8
Weighted averages		283 ± 3	321 ± 1	249 ± 5	287 ± 4

IV. DISCUSSION

A major result is that the rotational temperatures of the hydroxyl radicals at the peak of their production are related to the temperature of the liquid squalane surface. This is a strong indication that at least some of the hydroxyl radicals are temporarily trapped at the surface and at least partially adapt to its temperature. However, the fact that a surface temperature change is not fully reflected in the corresponding rotational temperature of the hydroxyl radicals indicates that some of them escape without being accommodated at the surface. This would be consistent with a second contribution from a direct abstraction mechanism. We note that in the absence of surface-temperature-dependent measurements in our previous preliminary report[44] we were only able to identify definitively the involvement of the transient trapping component.

This combination of trapping desorption and direct mechanisms is further supported by the fact that the rotational temperature of the products in $(v'=1)$ is moderately colder than in $(v'=0)$. Clearly, no significant difference would be expected between these temperatures if all the hydroxyl radicals in both vibrational levels were to be trapped and fully relax at the surface. This indicates at least a partial direct component. On the other hand, a larger temperature difference between $(v'=0)$ and $(v'=1)$ has been observed in the corresponding homogeneous gas-phase reaction.[22,51] Although it is admittedly a somewhat less direct argument, it is also reasonable to conclude that some of the products have had their rotational temperatures moderated towards that of the surface due to being trapped.

We have verified that it is possible to reproduce reasonably accurately the overall rotational distributions from reaction at the liquid surface by constructing weighted sums of two distributions, one at the surface temperature and the other that measured from the homogeneous gas-phase reaction with cyclohexane. Any quantitative significance of the weightings is certainly debatable, due to the relatively modest differences in the distributions and the combined uncertainties in the experimental data. Nevertheless, we note that the best agreement is generally found when the contributions are approximately equal, but with, if either, a predominance of the thermal (trapping-desorption) contribution. We note also that this ''branching'' is specific to the particular time delay at which it was measured.

As described in the introduction, our own work is predated by the complementary molecular-beam scattering measurements of Minton and co-workers.[6–8] They have previously reached the same conclusion that there are two mechanistic contributions on the basis of product velocities, i.e., *translational* energy and angular scattering distributions. It is interesting but probably not unexpected that these persist in our observations of *rotational* state distributions, because it is well established that in many collisional environments the translational and rotational degrees of freedom rapidly equilibrate. We would therefore expect the translational and rotational temperatures of the trapping-desorption component to be similar and close to the surface temperature (although no such similarity is required or even likely in the direct component).

Taken in isolation, we do not believe that the appearance profiles we have measured (see Fig. 2) could be deconvoluted reliably to extract independent estimates of product translational energies in our own experiments. However, if we adopt for the sake of argument some constraints imposed by the much more definitive molecular beam scattering measurements,[6–8] it is possible to check that there is at least a reasonable degree of consistency. We have attempted this by forward-simulating expected appearance profiles in a Monte Carlo fashion. The distributions sampled covered both geometric factors and speed distributions. Each simulation typically involved sampling 20 000 Monte Carlo ''trajectories.'' The volume over which $O(^3P)$ is produced by the photolysis laser can be assessed, as can the contributing area of liquid-surface covered wheel. A trajectory was considered successful if the OH product entered the region where it would be observed effectively by the probe laser/light guide combination. The $O(^3P)$ atom speed distribution from 355 nm photolysis of room-temperature NO_2 is known.[47] As noted above, this is broad, with an average speed of $1340\ ms^{-1}$. This turns out, in fact, to be the dominant overall broadening factor in our experiment. The β parameter of $+0.7$ is also known and was applied in conjunction with the relevant photolysis laser linear polarization to generate the appropriate angular distribution. We note that we did not impose an excitation function for $O(^3P)$ atom reactivity at the surface, since the form of this is essentially unknown.

We then made the necessary further assumptions that were guided by the work of Minton and co-workers.[6–8] The trapping-desorption product component was taken to have a Boltzmann-like velocity distribution distributed with a cosine weighting about the surface normal. The directly scattered component, in contrast, had an imposed angular distribution with a $\cos^4\theta$ weighting about a direction deviating in a specific way from the specular angular, mimicking the previous observations. The translational energies of the direct component further assumed quasielastic scattering with a surface of effective mass 76 amu.

On this basis, we have generated the quite plausible appearance profiles superimposed on the experimental data in Fig. 2. An important point is that we have used only a single adjustable parameter to vary the ratio of trapping desorption to direct components at the three independent laser axis-surface distances. There has been no rescaling of the relative magnitudes of the predicted or observed signals at these three distances, which were each normalized to that at the shortest distance. The fact that the trends in the magnitudes of the signals are reproduced very satisfactorily is therefore significant.

There is obviously an increasing discrepancy between the simulated and observed profiles at longer times. However, we do not necessarily believe this reveals any fundamental problem with the simulation procedure. By construction, the simulations do not include the possible effect of any secondary gas-phase collisions. However, as discussed above, the experimental conditions were designed to ensure a modest fraction of these collisions only over the earlier time periods. The greater observed persistence of OH signals at longer times, where it becomes increasingly likely that molecules will have suffered a secondary collision, would be consistent with the consequent reduction in the rate of escape from the observation zone.

Fitting to the magnitude of the profile in the region around its peak, we find that the optimum ratio of the two components is around 60:40 (in terms of total area) in favor of the thermal contribution. Considerable caution should certainly be applied before assigning much significance to the accuracy of this estimate. We have not yet made any of the necessary further detailed corrections, such as a flux-density transformation, for example. Nevertheless, it is in crude terms qualitatively consistent with our independent assessment above of the relative contributions based on rotational distributions. In particular, and probably the most important result arising from these simulations, the sharp rising edges at the earliest times can *only* be reproduced by assuming a significant fraction of a hyperthermal component. This is likely to remain true regardless of refinements of the simulation procedure and is further quite convincing support for a partial contribution from a direct scattering mechanism.

Our current measurements are clearly not particularly well designed to assess product velocity distributions, which are much better extracted from the molecular-beam scattering experiments. On the other hand, the state-specific spectroscopic basis of our method does naturally allow the definitive new observation that some of the hydroxyl radicals that escape the surface are vibrationally excited, which was not inferred previously.[6–8] As we have already noted,[44] this provides some indication of an upper limit on the duration of trapping-desorption component of the mechanism, on the ba-

sis of a comparison with the competitive rate of OH vibrational relaxation. A similar argument can be made for the survival of *any* OH, including the majority ($v'=0$) product, by comparison with the likely rate of secondary reaction. It is already established from the molecular-beam scattering experiments[6–8] that some H_2O is produced in the reaction, with similar characteristics of both direct and trapping-desorption contributions to its production. Rate constants for (thermal, and therefore almost entirely $v=0$) OH reaction with the largest tabulated gas-phase hydrocarbon, *n*-hexadecane, are of the order of 2×10^{-11} $cm^3\,s^{-1}$.[52] This is a factor of around ~15 times smaller than a typical total gas-kinetic rate constant for all collisions. In other words, those OH($v=0$) radicals that escape into the gas phase are unlikely to have experienced substantially more than ~15 secondary encounters with squalane molecules in the surface. Returning to the previous argument, this number will, in anything, be smaller for OH($v=1$). This is both because of a likely dynamical enhancement in its reactivity and because of the additional channel for nonreactive vibrational relaxation. It does not, however, currently seem to be possible to make this argument any more quantitative. As far as we are aware, there are no direct measurements of OH vibrational relaxation in condensed hydrocarbon phases. There are also perhaps rather surprisingly few for hydrocarbons in the gas phase. The only quantitative data we have located are for methane itself,[53] where the reaction and vibrational relaxation channels contribute approximately equally for OH($v=1$). However, the absolute reaction rate constants are much slower than for the larger hydrocarbons and in any case there is no reason to expect that the branching fraction between reaction and relaxation is transferable between systems.

We have previously alluded[44] to the possibility that the observation of OD ($v'=1$), now quantified and reinforced in the current study by the related results for OH, may itself provide some indirect evidence for the structure of the squalane surface. The basis of this argument is that it is very well established from the homogeneous gas-phase reactions[19] that there is a strong correlation between the nature of the C–H bond from which the H atom is abstracted and the degree of OH product vibrational excitation. Primary C–H units produce effectively negligible (immeasurably low) branching to OH ($v'=1$), with the proportion increasing rapidly in the sequence primary$<$secondary$<$tertiary. It is not feasible to extend this to a quantitative argument in which we might convert our measured phenomenological branching ratio to a ratio of sites from which the H atom has been abstracted. This is not least because there are no gas-phase data for hydrocarbons of a directly comparable size, but also because of considerable scatter in the reported ratios for those that have been studied.[19] Nevertheless, we reiterate our belief that it is very likely at least some of the OH (and OD) we observe must have come from secondary and/or tertiary sites along the squalane backbone. This is interesting because the limited information that is available on the structure of straight-chain hydrocarbon liquids, based on molecular dynamics simulations of normal C_{10} and C_{20} hydrocarbons,[33] suggests that the outer surface has an excess of $-CH_3$ endgroups. There are a number of reasons why this may not apply to squalane, most notably because of its branched-chain structure, and indeed more recent independent molecular dynamics calculations[34] do not identify a large excess.

Nevertheless, it suggests that a more definitive future experiment, perhaps involving deuterium labeling at selected positions along the chain of squalane or other selected hydrocarbons, might provide some new insight into the ordering in the surface layer and its ability to be penetrated by an attacking atom such as $O(^3P)$.

ACKNOWLEDGMENTS

The authors acknowledge the Verband der Chemischen Industrie for a scholarship (S.P.K.K.) and the UK EPSRC for a research grant and studentship (M.A.).

[1] I. Langmuir, Trans. Faraday Soc. **17**, 621 (1922).
[2] C. T. Rettner and D. J. Auerbach, Science **263**, 365 (1994).
[3] M. E. Saecker, S. T. Govoni, D. V. Kowalski, M. E. King, and G. M. Nathanson, Science **252**, 1421 (1991).
[4] G. M. Nathanson, P. Davidovits, D. R. Worsnop, and C. E. Kolb, J. Phys. Chem. **100**, 13007 (1996).
[5] A. J. Kenyon, A. J. McCaffery, C. M. Quintella, and M. D. Zidan, Chem. Phys. Lett. **190**, 55 (1992).
[6] D. J. Garton, T. K. Minton, M. Alagia, N. Balucani, P. Casavecchia, and G. G. Volpi, Faraday Discuss. Chem. Soc. **108**, 387 (1997).
[7] D. J. Garton, T. K. Minton, M. Alagia, N. Balucani, P. Casavecchia, and G. G. Volpi, J. Chem. Phys. **112**, 5975 (2000); **114**, 5958 (2001).
[8] J. Zhang, D. J. Garton, and T. K. Minton, J. Chem. Phys. **117**, 6239 (2002).
[9] A. K. Bertram, A. V. Ivanov, M. Hunter, L. T. Molina, and M. J. Molina, J. Phys. Chem. A **105**, 9415 (2001).
[10] T. Moise and Y. Rudich, Geophys. Res. Lett. **28**, 4083 (2001).
[11] T. L. Eliason, J. B. Gilman, and V. Vaida, Atmos. Environ. **38**, 1367 (2004).
[12] L. J. Leger and J. T. Visentine, Aerosp. Am. **24**, 32 (1986); J. Spacecr. Rockets **23**, 505 (1986); L. E. Murr and W. H. Kinnard, Am. Sci. **81**, 152 (1993).
[13] A. Hori, S. Takamuku, and H. Sakurai, J. Org. Chem. **42**, 2318 (1977).
[14] E. Zadok and Y. Mazur, J. Org. Chem. **47**, 2223 (1982); Angew. Chem., Int. Ed. Engl. **21**, 303 (1982).
[15] P. Patiño, F. E. Hernández, and S. Rondón, Plasma Chem. Plasma Process. **15**, 159 (1995).
[16] J. T. Herron, J. Phys. Chem. Ref. Data **17**, 967 (1988).
[17] N. Cohen and K. R. Westberg, J. Phys. Chem. Ref. Data **20**, 1211 (1991).
[18] Y. Rudich, Y. Hurwitz, S. Lifson, and R. Naaman, J. Chem. Phys. **98**, 2936 (1993).
[19] F. Ausfelder and K. G. McKendrick, Prog. React. Kinet. **25**, 299 (2000).
[20] P. Andresen and A. C. Luntz, J. Chem. Phys. **72**, 5842 (1980).
[21] N. J. Dutton, I. W. Fletcher, and J. C. Whitehead, Mol. Phys. **52**, 475 (1984).
[22] G. M. Sweeney, A. Watson, and K. G. McKendrick, J. Chem. Phys. **106**, 9172 (1997).
[23] F. Ausfelder, H. Kelso, and K. G. McKendrick, Phys. Chem. Chem. Phys. **4**, 473 (2002).
[24] H. Tsurumaki, Y. Fujimara, and O. Kajimoto, J. Chem. Phys. **112**, 8338 (2000).
[25] A. C. Luntz and P. Anderson, J. Chem. Phys. **72**, 5851 (1980).
[26] S. P. Walch and T. H. Dunning, Jr., J. Chem. Phys. **71**, 3221 (1980).
[27] C. Gonzales, J. J. W. McDouall, and H. B. Schlegel, J. Phys. Chem. **94**, 7467 (1990).
[28] J. C. Corchado, J. Espinosa-García, O. Roberto-Neto, Y.-Y. Chuang, and D. G. Truhlar, J. Phys. Chem. A **102**, 4899 (1998).
[29] M. Gonzáles, J. Hernando, J. Millán, and R. Sayós, J. Chem. Phys. **110**, 7326 (1999).
[30] D. C. Clary, Phys. Chem. Chem. Phys. **1**, 1173 (1999).
[31] J. Palma and D. C. Clary, J. Chem. Phys. **112**, 1859 (2000); **115**, 2188 (2001).
[32] H.-G. Yu and G. Nyman, J. Chem. Phys. **112**, 238 (2000).
[33] J. G. Harris, J. Phys. Chem. **96**, 5077 (1992).

[34] C. D. Wick, J. I. Siepmann, and M. R. Schure, Anal. Chem. **74**, 3518 (2002).
[35] G. Li, S. B. M. Bosio, and W. L. Hase, J. Mol. Struct. **556**, 43 (2000).
[36] D. Troya and G. C. Schatz, 9th International Symposium on Materials in a Space Environment, ESA, SP-540, 121, 2003.
[37] D. Troya and G. C. Schatz, J. Chem. Phys. **120**, 7696 (2004).
[38] B. S. Day, S. F. Shuler, A. Ducre, and J. R. Morris, J. Chem. Phys. **119**, 8084 (2003).
[39] M. K. Ferguson, J. R. Lohr, B. S. Day, and J. R. Morris, Phys. Rev. Lett. **92**, 073201 (2004).
[40] K. D. Gibson, N. Isa, and S. J. Sibener, J. Chem. Phys. **119**, 13083 (2003).
[41] Y. Paz, S. Trakhtenberg, and R. Naaman, J. Phys. Chem. **98**, 13517 (1994).
[42] A. J. Wagner, G. M. Wolfe, and D. H. Fairbrother, J. Chem. Phys. **120**, 3799 (2004).
[43] X. Qin, T. Tzvetkov, and D. C. Jacobs, Nucl. Instrum. Methods Phys. Res. B **203**, 130 (2003).
[44] H. Kelso, S. P. K. Köhler, D. A. Henderson, and K. G. McKendrick, J. Chem. Phys. **119**, 9985 (2003).
[45] M. P. Sinha and J. B. Fenn, 5th International Symposium on Molecular Beams, Nice, 1975.
[46] S. L. Lednovich and J. B. Fenn, AIChE J. **23**, 454 (1977).
[47] R. P. Baker, M. L. Costen, G. Hancock, G. A. Richie, and D. Summerfield, Phys. Chem. Chem. Phys. **2**, 661 (2000).
[48] J. Luque and D. R. Crosley, SRI International Report MP 99-009, 1999.
[49] D. R. Yarkony, J. Chem. Phys. **97**, 1838 (1992).
[50] K. M. Hickson, C. M. Sadowski, and I. W. M. Smith, Phys. Chem. Chem. Phys. **4**, 5613 (2002).
[51] F. Ausfelder, H. Kelso, and K. G. McKendrick, Phys. Chem. Chem. Phys. **4**, 473 (2002).
[52] R. Atkinson, J. Phys. Chem. Ref. Data **26**, 215 (1997).
[53] K. Yamasaki, A. Watanabe, T. Kakuda, N. Ichikawa, and I. Tokue, J. Phys. Chem. A **103**, 451 (1999).